Article:
Petersen, Anne Ugleholdt, Jevric, Martyn, Mandle, Richard J orcid.org/0000-0001-9816-9661 et al. (5 more authors) (2017) Photoswitching of Dihydroazulene Derivatives in Liquid-Crystalline Host Systems. Chemistry : A European Journal. pp. 5090-5103. ISSN 1521-3765

https://doi.org/10.1002/chem.201700055

Photoswitching of Dihydroazulene Derivatives in Liquid Crystalline Host Systems

Anne Ugleholdt Petersen,[a] Martyn Jevric,[a] Richard J. Mandle,[b] Mark T. Sims,[b] John N. Moore,[b] Stephen J. Cowling,[b] John W. Goodby,[b] and Mogens Brøndsted Nielsen*[a]

Abstract: Photoswitches and dyes in the liquid crystalline nematic phase have the potential for use within a wide range of applications. A high order parameter is desirable in order to maximize the change in properties induced by an external stimulus. A set of photochromic and non-photochromic dyes were investigated for these applications. It was found that a bent-shaped 7-substituted dihydroazulene (DHA) photoswitch exhibited liquid crystalline properties. Further investigation demonstrated that this material actually underwent two distinctive reaction pathways upon heating to a deactivated form via a 1,5-sigmatropic shift and to a linear 6-substituted DHA. In addition, elimination of hydrogen cyanide from these photoactive DHAs gave both bent and linear azulene dyes. In a nematic host, which has no absorbance around 350 nm, it was found that only the linearly shaped DHA derivative possessed nematic properties; however, both 6- and 7-substituted DHAs were found to have high order parameters. In the nematic host, ring opening of either DHA to the corresponding vinylheptafulvene (VHF) resulted in a decrease in dichroic order parameter and an unusually fast back reaction to a mixture of both DHAs. Likewise, only the linearly shaped azulene derivative showed mesomorphic properties. In the same nematic host, high order parameters were also observed for these dyes.

Introduction

Molecular photoswitches have been classified as being either P-type, where inter-conversion between two states can be facilitated in both directions using light, or as T-type, in which thermal energy can be used to achieve a back reaction.[1] Further, some photoswitches can be both P- and T-type, such as spiropyrans and azobenzenes.[1] Use of photoswitches in liquid crystal technology has shown potential for controlling the macrostructure of liquid crystals, which has amongst others shown applications in holographic image storage, for which photoswitches that undergo extremely slow back reactions in a liquid crystal host are desirable.[2] The properties of the photoswitch may also be used to modulate the amount of light passing through a sample on account of a change in the chromophoric properties, which is of relevance in eye wear technologies.[3] Another topic of interest within the field of liquid crystal technology is liquid crystal host systems doped with guest dyes,[4] where the absorbance of polarized light is different when parallel and perpendicular to the host director. Such devices have a wide range of potential applications including possible applications in displays,[5] high performance thin-film polarizers,[6] optically controlled diffraction gratings,[7] security devices,[8] switchable solar windows,[9] and 3D imaging for biological applications.[10] The degree to which alignment occurs is described by the dichroic order parameter, which is a measure of how well the dye aligns with the director for the liquid crystal, and how well the transition dipole moment is aligned with the long axis of the dye molecule.[4, 11]

The dihydroazulene (DHA) **1** presents an example of a T-type photochrome, which upon irradiation opens to a vinylheptafulvene (VHF) **2**.[12] As the VHF is not affected by visible light, full conversion to VHF in solution is possible and is not complicated by photostationary states. VHF converts back to DHA thermally, with a rate depending on the solvent polarity, the temperature, and the DHA substituent pattern.[13, 14] Of particular interest in this system are the large structural and electronic differences between the DHA and VHF, where VHF is very polar on account of strong resonance contributors of a zwitterion having tropylium coupled with "malonitrile anion character" as shown in Scheme 1. DHA and VHF differ significantly in their absorption spectra. In solution the DHA form appears yellow, while the VHF is intensely red in color. Lastly, there is a structural reorganization in the molecule going from DHA to VHF, and VHF is most stable as its s-*trans* conformer **2b** (Scheme 1). Many structural modifications have been made to DHA altering the rate of the back reaction,[14-16] but to date there are no DHA derivatives whose VHF form is long-lived enough for potential use in holographic storage, while at the same time showing high stability.

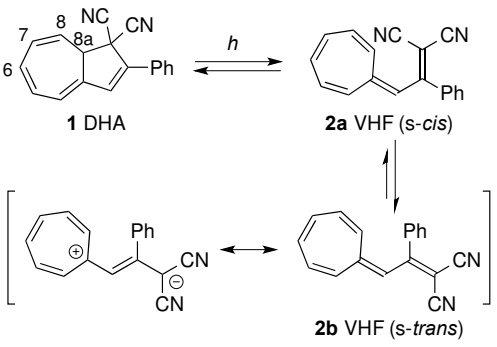

Scheme 1. DHA/VHF photo-/thermoswitch showing the ring-opening to s-*cis* VHF, and the more stable s-*trans* conformer. Relevant positions on the DHA are numbered.

In a previous study, we have reported that DHAs **3** and **4**, which are both substituted with biaryl units (Figure 1), exhibited

[a] Dr. A. U. Petersen, Dr. M. Jevric, Prof. Dr. M. B. Nielsen
Department of Chemistry
University of Copenhagen
Universitetsparken 5, DK-2100 Copenhagen Ø
E-mail: mbn@chem.ku.dk
[b] Dr. R. J. Mandle, Dr. M. T. Sims, Dr. J. N. Moore, Dr. S. J. Cowling, Prof. Dr. J. W. Goodby
Department of Chemistry
University of York
Heslington, York, YO10 5DD, UK

Supporting information for this article is given via a link at the end of the document

mesophases not far above room temperature.[17] The core DHA structure is rod-shaped, which is a desirable quality for forming the nematic phase. However in the nematic phase, full conversion to the VHF had not been possible, but photolysis of **4** did, however, result in annihilation of the defects and established a higher degree of order within the resulting mesophase when the VHF underwent ring-closure back to **4**.[17] Synthetic developments in the chemistry of DHA have allowed for the introduction of aromatic substituents at the 7-position.[18, 19] However, placing a substituent at this position on the seven-membered ring becomes complicated as when performing switching experiments in solution, an isomeric scrambling giving DHAs with the substituents in either the 6- or 7-positions can occur after one ring-opening/closure cycle.[19] This is possible as the VHF has zwitterionic character, allowing rotation around the exocyclic olefin to form an isomeric *E*/*Z*-VHF mixture.[19] Nevertheless, attaching a substituent at the 7-position allows for the possibility of extending the results found for **3** by having alkyl chains on both ends of this rod-shaped motif. Thus the aim of this study was to extend our initial findings by introducing a second octyloxyphenyl unit to the 7-position and assessing its properties both neat and incorporated into a guest-host system and studying how it is affected by a photo-thermal cycle and subsequent ring closure in regard to the order parameter. Interestingly, it has been found that DHA can be encouraged to undergo the elimination of hydrogen cyanide to form the corresponding 1-cyanoazulene.[20] Azulenes are strong chromophores, which is the result of a high degree of polarization of the bicyclic motif, and they have therefore attracted attention as dyes for guest-host systems, but to date their potential for use has been limited because of low order parameters.[21] The current work has therefore also focused upon the order parameter properties arising from having a nitrile in the 1-position.

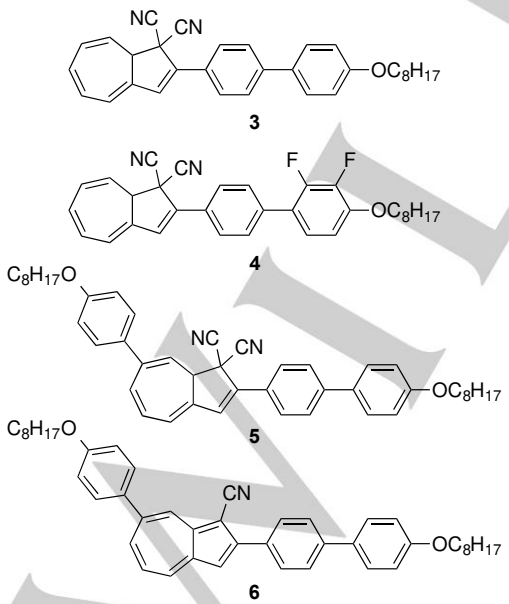

Figure 1. Chemical structures of DHAs **3** and **4** previously shown to exhibit liquid crystalline properties, and the chemical structures of **5** and **6** used in the present work.

Here we present studies of the properties of guest-host materials of DHA **5** in a bicyclohexyl host, which has a nematic phase at room temperature, and we report the behavior of the components of this dynamic system throughout a photo-thermal cycle. In addition, azulene derivative **6** was conveniently prepared from **5**, and the dichroic order parameters for the molecular components of **5** and **6** were determined in aligned cells.

Results and Discussion

Synthesis and Physical Properties. DHA **5** was synthesized according to Scheme 2, and for comparative purposes the analogue **7** with no alkoxy substituents on the phenyl groups was also made. Both these DHAs could be synthesized from iodo-substituted DHA **8** via a previously reported bromination-elimination protocol,[18] which allowed for the regioselective introduction of a reactive vinyl bromide to the 7-position (compound **9**). After a two-fold palladium catalyzed Suzuki coupling, purification of products **5** and **7** involved flash column chromatography followed by crystallization. The low yield attributed to **7** included the isolation of significant amounts of azulene byproducts. Azulene formation by elimination of HCN is known to occur under cross-coupling conditions,[18] and in this case the product mixture was complicated also by debromination of **9**. In the ^{1}H NMR spectrum, a DHA without a substituent upon the seven-membered ring exhibits an apparent doublet of triplets for the 8a proton at ca. δ 3.7 ppm, whereas for **5** and **7**, now having a substituent in the 7-position, the multiplicity of this signal appears as a distinctive doublet of doublets.

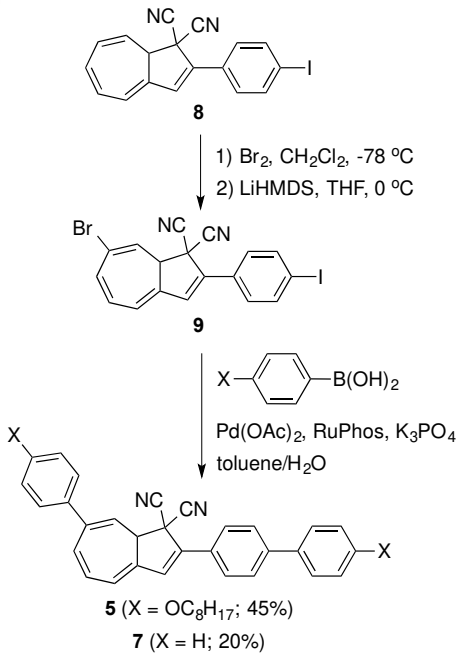

Scheme 2. Synthesis of DHAs **5** and **7** via a bromination-elimination protocol followed by a Suzuki cross coupling.

A preliminary investigation of **5** using polarized optical microscopy and differential scanning calorimetry (DSC) showed that events such as the melting point and appearance of the mesophase changed when cooling and heating the sample throughout several cycles in the absence of light (see SI). Using DSC in conjunction with NMR at different temperatures showed **5** to undergo conversion when heated to temperatures above 100 °C. Two distinctive reaction pathways seemed to occur; isomerization to the 6-substituted isomer **10** and reaction via a 1,5-sigmatropic shift furnishing compound **11** (Scheme 3). However, decomposition to unidentified products was evident when heating **5** above 180 °C. It is conceivable that the origin of **10** could arise from a ring-opening/closure cycle via a VHF intermediate. Product **11** is not photoactive as one requirement for the DHA to be photoactive is that the sp^3 carbon of the cycloheptatriene is in the 8a position. In order to probe whether these processes are specific to compound **5**, or more general for DHA, base system **7** was subjected to the same experiments. As DHA **7**, having no long alkyl substituents, presumably should not exhibit any liquid crystal properties, it can be shown that the formation of any possible liquid crystalline phases do not contribute to these isomerization processes. In this case, analogous products **12** and **13** were obtained, however in differing product ratios, as discussed below.

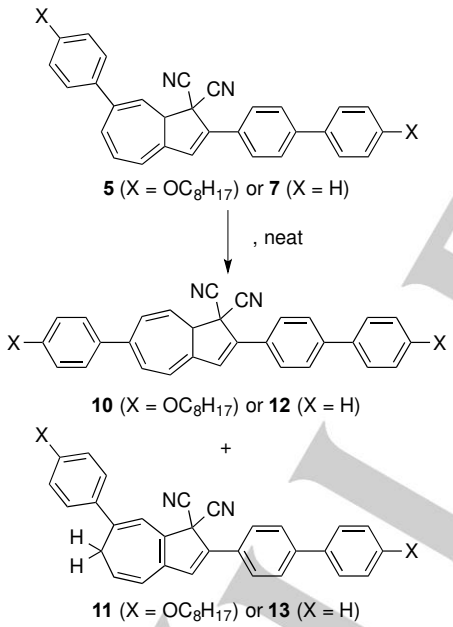

Scheme 3. Reactions of DHAs **5** and **7** when heated neat. For product ratios and yields, see Table 1.

Interest remained in the possibility of heating DHAs **5** and **7** on a preparative scale to selectively form single reaction products. The results of different heating experiments are summarized in Table 1. One strong motivation included the isolation of photoactive DHA **10**, which has the ideal properties for a liquid crystalline material and it would be desirable to determine its contribution in a device as it is expected to be present after a photo-thermal cycle. It was found that heating DHA **7** at 110 °C for one week gave a clean conversion to **13** (Entry 1). However, when **7** was subjected to 140 °C for several hours (Entry 2), a 5.6 mixture of **12** and **13** was obtained, whilst heating to 180 °C resulted in DHA **12** being the major product (Entry 3). Compound **13** exhibited very good thermal stability and was found to be stable above 200 °C. Conversely, heating **12** (see SI) showed evidence of conversion back to **7** in addition to **13**. These results suggest that an equilibrium exists between photoactive DHAs **7** and **12**; however, the 1,5-sigmatropic shift experienced by **7** is irreversible. No evidence was found pertaining to a 1,5-sigmatropic shift of **12**.

Interestingly, the opposite trend was observed for DHA **5**, where heating at a lower temperature favored DHA **10** (Entry 4), which could thereby be purified by careful chromatography. On the other hand, considerably more heat energy was required for the 1,5-sigmatropic shift to occur to form **11** and significant decomposition accompanied its formation (Entries 5 and 6). As observed with **13**, its analogue **11** was found to also be thermally stable though small amounts of decomposition could be observed by ^{1}H NMR spectroscopy, but in this case no evidence of formation of either **5** or **10** could be found. It appears that the electron-donating octyloxyphenyl contributes to the formation of the thermodynamic 6-substituted DHA **10** at lower temperatures, presumably by better stabilizing the VHF, while the sigmatropic shift has the lowest activation barrier for DHA **7**.

Table 1. Products obtained when heating either DHA **5** or **7** neat at given temperatures and times.[a]

Entry	DHA	Temperature (°C)	Time (h)	Product ratio[b]	Isolated yield
1	**7**	110	168	0:1 (**12**:**13**)	100% (**13**)
2	**7**	140	4.7	5:6 (**12**:**13**)	30% (**12**), 30% (**13**)
3	**7**	180	1	4:1 (**12**:**13**)	28% (**12**)
4	**5**	110	40	5:1 (**10**:**11**)	86% (**10**)
5	**5**	140	24	-[c]	16% (**11**), 24% (**5**/**10**)[d]
6	**5**	175	1	-[c]	7% (**11**)

[a] The heating was performed in a sealed vessel under argon in the dark. [b] Product ratio determined by ^{1}H NMR spectroscopy. [c] Not determined due to significant decomposition of the sample. [d] Ratio of 3:7 (**5**:**10**).

Azulenes usually form in small quantities when attempting to subject DHA to further functionalization under reaction conditions such as Suzuki and Sonogashira cross couplings. The most effective base to intentionally effect the formation of azulenes from DHA has been found to be 1,8-

diazabicyclo[5.4.0]undec-7-ene (DBU). It was thought that by eliminating hydrogen cyanide from both **5** and **10**, it may be possible to access dyes with mesomorphic properties. DHA **5** could be transformed into the corresponding azulene **6** in a low yield of 32% by treatment with an excess of DBU at room temperature (Scheme 4).

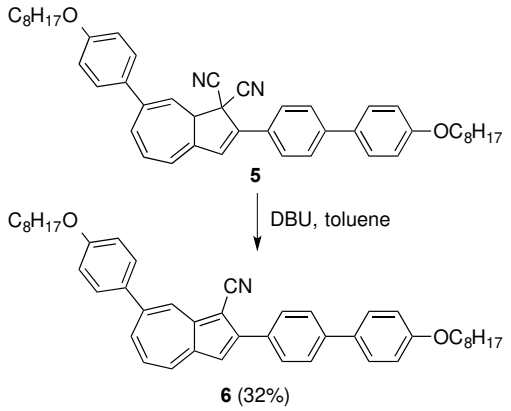

Scheme 4. Synthesis of azulene **6** by elimination of hydrogen cyanide from DHA **5**.

Azulene **14** was also synthesized from DHA **5**, using a two-step procedure (Scheme 5). As described above, heating a neat sample of **5** at 110 °C for 40 hours gave **10** in high yield. This was followed by elimination of hydrogen cyanide, made possible by addition of catalytic DBU and excess of hexamethyldisilazane (HMDS) to a toluene solution of **10**. HMDS was added to maintain the catalytic cycle of DBU and was also introduced as a potential cyanide scavenger. This protocol facilitated the formation of azulene **14**, which could be conveniently isolated by recrystallization following column chromatography. While azulene **6** was isolated as a blue-green solid, azulene **14** was a brown solid and appeared maroon in solution (UV-Vis absorption spectra are included in SI).

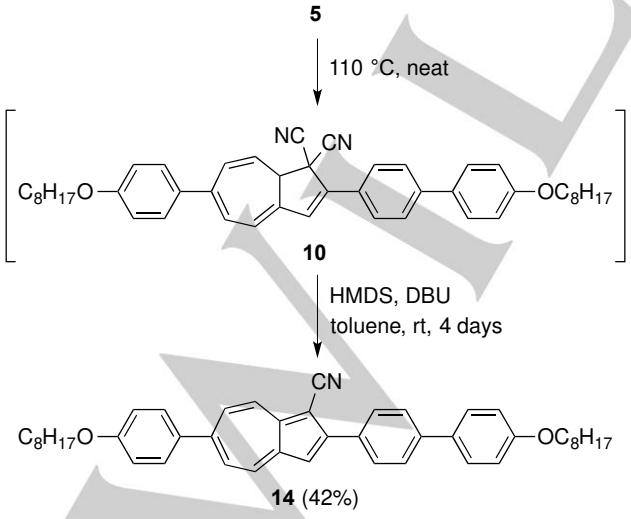

Scheme 5. Synthesis of azulene **14** from DHA **5** *via* formation of **10** as an intermediate.

Liquid-crystalline and Photoswitching Properties of DHAs 5 and 10. Since it was not possible to investigate the liquid crystalline properties of neat samples of **5** and **10**, they were both doped into a liquid crystalline host. To be compatible with the DHA/VHF couple, the host should have low absorbance around 350 nm (the region where DHA absorbs) and possess a nematic phase at ambient temperature in addition to the host being miscible with the dopants. Many commonly used hosts incorporate phenyl rings (*e.g.* E7; CAS# 63748-28-7) and so are not suitable due to absorbance in the near-UV. For this reason host **15** (for which the transition temperatures and composition are given in Figure 2) was employed as it has practically no absorbance above 300 nm

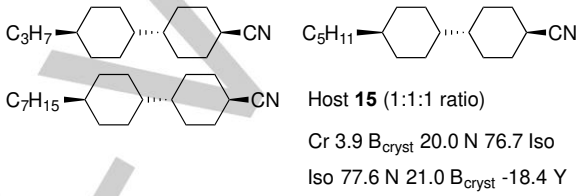

Figure 2. Composition and transition temperatures (°C) for liquid crystal host **15**.

Both DHAs **5** and **10** were individually doped into host **15** at five different concentrations and examined by polarized optical microscopy (POM) and DSC. The partial phase diagrams are shown in Figure 3. Assuming a linear relationship between $T_{N\text{-}Iso}$ and concentration, extrapolation of the clearing points for the nematic phase for **5** in **15** leads to a virtual nematic to isotropic (N-I) transition temperature of 17 °C for **5**, whereas using this method for compound **10** in host **15** gave a virtual N-I transition temperature of 84 °C. The increased thermal stability of the virtual nematic phase of **10** relative to **5** is likely to be a consequence of the linear molecular shape of the former, the latter being bent.

It is known that the VHF formed upon irradiation of a 7-aryl substituted DHA can undergo ring closure to a mixture of both 6- and 7-substituted isomers, usually in approximately the same ratio, although this ratio is specific to the substituent pattern of the DHA.[15d] As the reverse reaction for the DHA/VHF couple is thermally driven, this approach could not be used to determine the liquid-crystalline properties of the VHF. However, it was still important to construct a phase diagram of the DHA mixture after a successive photo-thermal cycle. Separate mixtures containing pure **5** in matrix **15** and another consisting of pure **10** also in matrix **15** were both irradiated to form VHFs (*E*/*Z* mixture), and then allowed to close back to a mixture of **5**/**10**. Upon irradiation, both **5** and **10** underwent ring-opening to VHFs having identical UV-Vis absorption profiles. Further inspection by UV-Vis absorption spectroscopy (described in the following section) showed that ring closure in the dark at room temperature from both mixtures gave the same ratio of **5** to **10**. Both sets of mixtures formed after irradiation of **5** or **10** were measured by DSC, and

the partial phase diagrams are shown in Figure 4. By extrapolation, this mixture of **5**/**10** exhibited a nematic phase with a clearing point at 33 °C. This was a substantially lower clearing point than for neat **10** in matrix **15** and higher than found for **5**. Knowing the individual virtual nematic-isotropic transition temperatures of **5** and **10** it is possible, assuming a linear relationship between concentration and these transition temperatures, to obtain a ratio for the mixture of **5**:**10**. By this method a value of 3:1 is obtained for the ratio of **5**:**10**, matching that found from the absorbance spectra, thus a clearing point of 33.5 °C for the pure mixture results from a ratio of 3:1 of **5**:**10**.

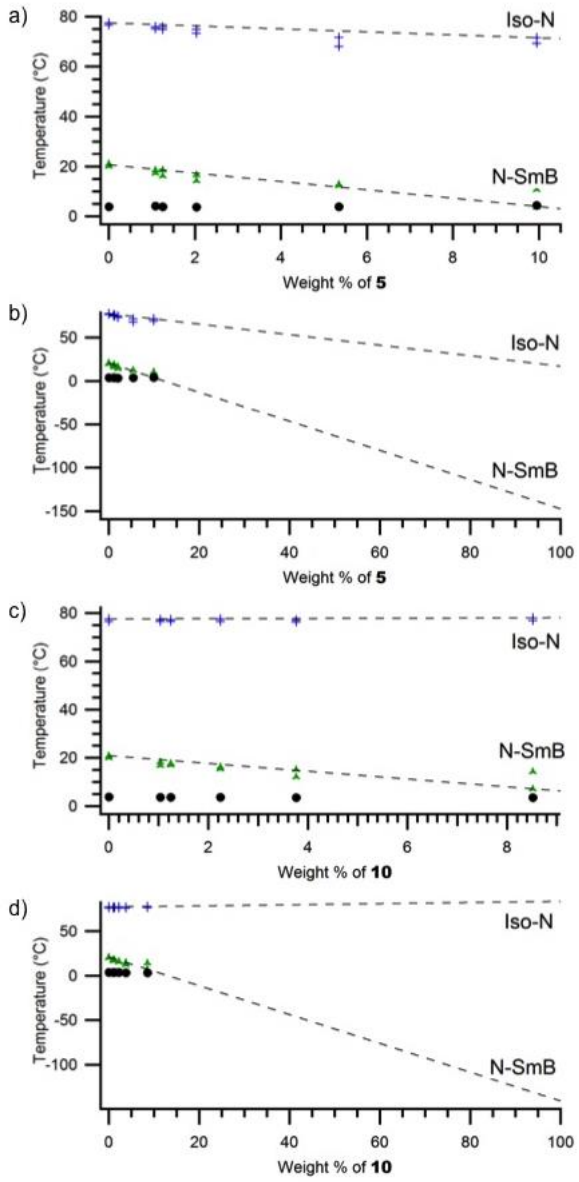

Figure 3. Partial phase diagrams for a) **5** in host **15** at different weight percentages, b) **5** extrapolated to weight percentage of 100%, c) **10** in host **15** at different weight percentages, d) **10** extrapolated to weight percentage of 100%.

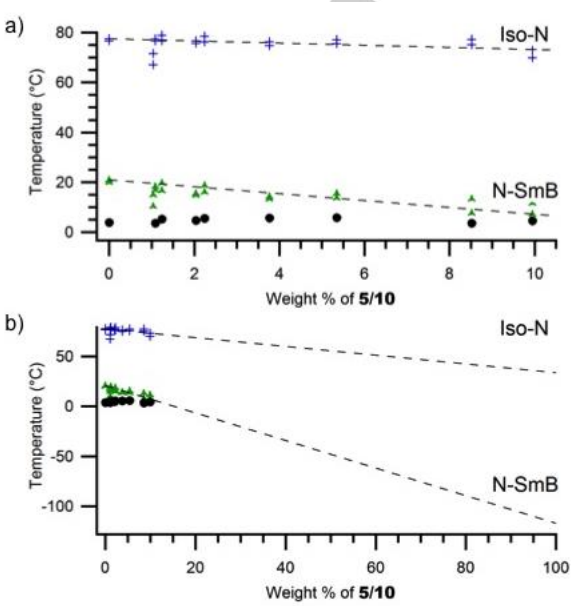

Figure 4. Partial phase diagrams a) for **5**:**10** in a ratio of 3:1 in weight percentages in host **15**, arising from irradiation of samples containing either **5** or **10**, giving the same ratio upon back reaction to the DHA, b) for **5**:**10** mixture extrapolated to weight percentage of 100%.

The dielectric properties of independent mixtures of **5** and **10** in host **15**, as well as the corresponding *E*/*Z* mixture of VHFs, and the **5**/**10** mixtures (obtained from ring closure of the corresponding VHFs), were also studied. These showed only small or no change in the dielectric anisotropy upon irradiation, going from the DHA to VHF (for more information, see SI).

Photochemical Properties. All photochromic DHAs made in this study were examined by UV-Vis absorption spectroscopy in acetonitrile, which included measuring the kinetics of the back reaction for the conversion of the VHFs to their respective DHAs. When irradiated with light, the DHAs opened to their corresponding VHFs (Figure 5), which ultimately closed to afford mixtures of the 7-substituted and 6-substituted DHA isomers (Scheme 6). This being said, they opened to the same mixtures of VHFs, as shown by the matching absorption spectra and the same resultant mixtures of DHAs, shown in Scheme 6. Thus, DHAs **5** and **10** opened to VHF **16** (*E*/*Z*) and closed to **5**/**10** in the same ratio, irrespective of whether one started the measurement with either **5** or **10**. The same was the case for the system **7**/**12**.

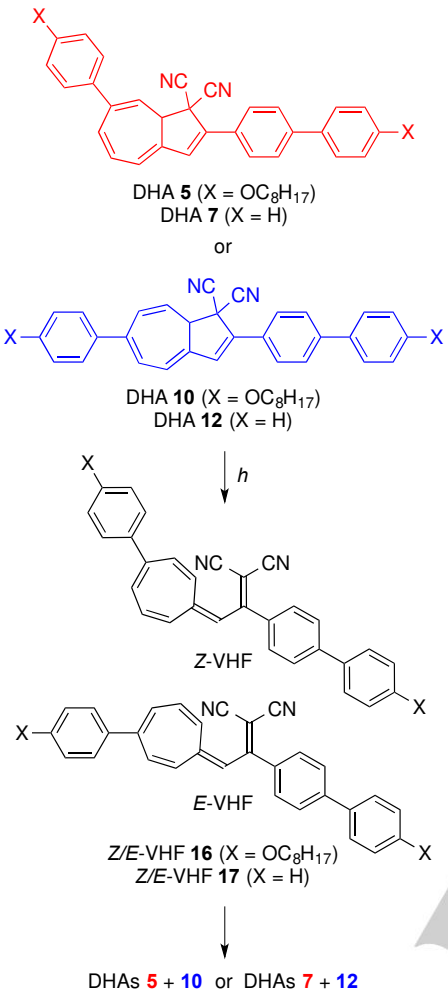

Scheme 6. Ring-opening/closure cycles of DHA couples **5**/**10** and **7**/**12**.

Table 2. Absorption maxima (λ_{max}) for DHAs and VHFs in acetonitrile and in host **15**. Rate constants (k) and associated half-lives ($t_{1/2}$) at 25 °C of the back reactions (VHF to DHA mixture) are also listed.

Starting compd	Medium	k [a] (10^{-5} s^{-1})	$t_{1/2}$ (min)	λ_{max} (DHA) (nm)	λ_{max} (VHF) (nm)	λ_{max} (DHA mixture) (nm)
7	CH_3CN	5.52	209	367	492	375
12	CH_3CN	5.51	210	389	492	375
5	CH_3CN	9.20	126	374	508	383
10	CH_3CN	9.24	125	402	508	383
5	Host **15** [b]	65.7	18	379	505	382
10	Host **15** [b]	66.1	18	407	505	382
5	Host **15** [c]	62.2	19	378	505	382

[a] Rate constant for the thermal back reaction measured at 25 °C unless otherwise stated. [b] Measured in a homogenously aligned cell at ambient temperature. [c] Measured in an unaligned cell at ambient temperature.

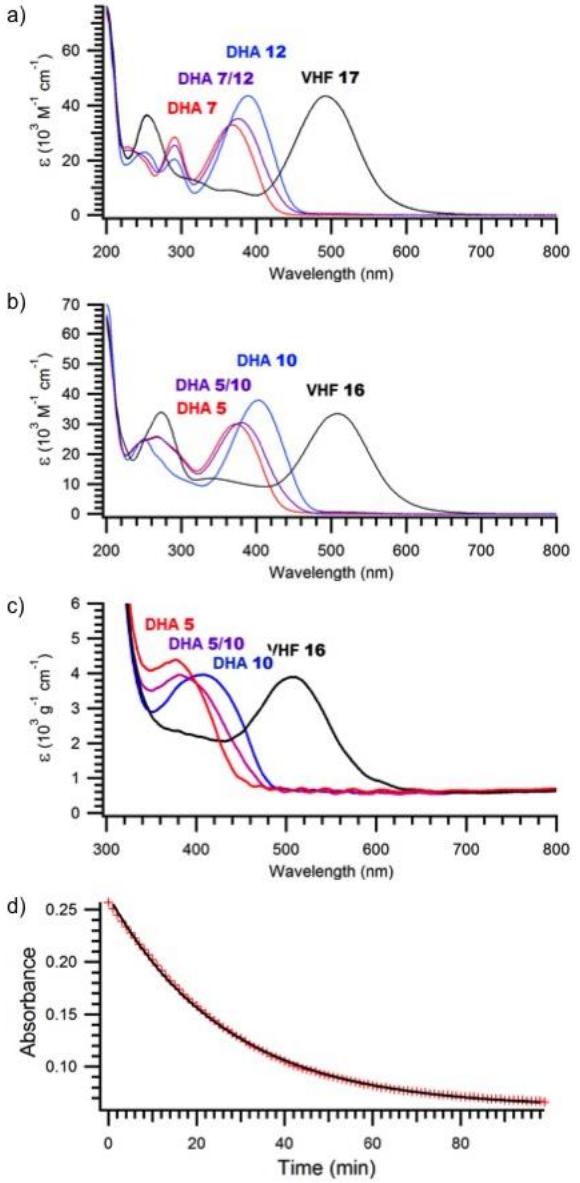

Figure 5. UV-Vis absorption spectra of a) DHAs **7**, **12**, **7**/**12** and VHF **17** in acetonitrile, b) DHAs **5**, **10**, **5**/**10** and VHF **16** in acetonitrile, c) DHAs **5**, **10**, **5**/**10** and VHF **16** in host **15**; as the density is not known for this blend, the extinction coefficient is reported with the unit of $g^{-1}cm^{-1}$. For ease of comparison, molar absorptivities are plotted in the figures for both pure compounds and mixtures. d) Decay of absorption of **16** in host **15** at λ_{max} = 505 nm at ambient temperature (including a first-order kinetics fit).

The absorption spectra for DHAs **5** and **10** and kinetics data for the VHF to DHA back reactions were measured individually in acetonitrile. In both cases, under irradiation they opened to the VHF **16**, giving the same spectrum (Figure 5b and Table 2). In the dark, VHF **16** closed to a mixture of **5**/**10** in an estimated ratio of 7:3, with a rate constant of 9.2 x 10^{-5} s^{-}

[1] following 1st order kinetics. The ratio of **5**/**10** was determined from the contributions of known absorption spectra of pure **5** and **10**. Having an electron-donating group at either the 6- or 7-position indeed speeds up the rate of the back reaction, which may be attributed to it stabilizing the zwitterionic transition state. Although there is the same electron-donating group on the 2-position, the substituent at this position also contains a bridging phenyl group diminishing its influence. This is evidenced by the parent system, which has a slower rate of ring-closure and itself gives a mixture of 6- and 7-substituted isomers.

UV-Vis absorption studies were also carried out on **5** and **10** in the nematic host medium **15** at ambient temperature, for which the absorption spectra can be seen in Figure 5c. These were measured in a homogenously aligned cell at values of λ > 340 nm, owing to the indium tin oxide (ITO) coating on the glass that the cell was made from. Again ring opening of the independent mixtures of DHAs **5** and **10** gave VHF **16**, and upon ring closure the same absorption maximum was observed for the resulting mixture of **5**/**10**, which was found to be formed in ratio of 3:1 (determined in the same fashion as explained earlier) which was in agreement with the phase diagrams. It was found that the rate of the ring closure of **16** was significantly faster in the nematic phase of host **15** than in acetonitrile, with a rate constant of 6.6 x 10^{-4} s^{-1}. This large increase in reaction rate could be explained by the effect of the nematic material impacting the VHF **16**, driving ring closure to DHA **5**/**10** to form a structure that is less disruptive to the orientational order of the nematic host. The nematic host could as well be affecting the s-*trans* and s-*cis* conformer equilibrium of VHF. As the VHF is less rod like in the core structure, it seems possible that the VHF could be destabilized in the nematic host, relative to in solution, contributing to an enhanced rate of ring closure. Surprisingly, DFT calculations (B3LYP/6-31G(d)) comparing the dipole moments of host **15** (4.56 Debye) to acetonitrile (3.81 Debye) showed that **15** was more polar, and this should thus also be considered as one factor to the faster ring closure of VHF **16** in the nematic host (since ring closure is promoted in polar media[13]). The measurement was performed in homogeneously aligned cells, and it was thought that the long range order would not have any effect on the kinetics. However, in order to verify this assumption, the measurement was repeated in an unaligned cell, which gave similar results.

Studies of DHAs **5** and **10** in the aligned cells were also used to examine how well both the DHAs and VHFs align with host **15**. In order to obtain the experimental order parameter for the DHAs and VHFs in host **15**, the absorption spectra were measured with the incident light polarized parallel and perpendicular to the alignment of the cell (Figure 6). From these spectra, it is clear that the DHAs **5** and **10** are more aligned within the host than *E*/*Z*-VHF **16**. The dichroic order parameters determined from the spectra in Figure 6 are given in Table 3. The molecule with the greatest degree of linearity, **10**, has a higher order parameter than the bent molecule **5**, while it is clear that the VHF is poorly aligned. This implies that DHAs **5** and **10**, and the mixture **5**/**10** in host **15** should be responsive to the application of an electric field. Incorporation of such a composite material into a device gives the possibility of regulating the passage of light through a cell containing the DHA form in host **15** by turning on and off an electric field; however, this possibility is not available in the VHF form.

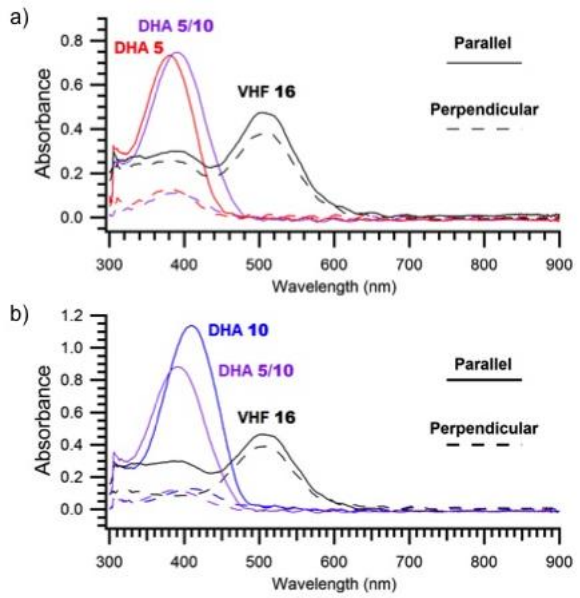

Figure 6. Absorption spectra in liquid crystal host **15**, with the light polarized parallel and perpendicular to alignment, of a) DHA **5** and the corresponding VHF **16** and the mixture of **5**/**10** formed upon closing of **16**, b) DHA **10** and the corresponding VHF **16** and the mixture of **5**/**10** formed upon closing of **16**.

Table 3. Order parameters (*S*) for DHAs **5** and **10** in host **15** before, during and after irradiation.

Starting compound	**5**	**10**
Before irradiation	0.62	0.72
During irradiation	0.07	0.06
After irradiation	0.66	0.69

Density functional theory (DFT) optimizations and time-dependent DFT calculations were carried out for the ethoxy-substituted analogs of DHAs **5** and **10** and VHF **16**, hereon denoted by **5'**, **10'** and **16'**, in order to determine the angle, β, between the minimum moment of inertia (MOI) axis and the electronic transition dipole moment (TDM) vector associated with the longest wavelength transition of significant oscillator strength. These calculations (see Table 4) in essence can give an indication of how well the TDM is aligned with the long axis for each molecule.[22] For **5'**, this angle was calculated to be

9.4° and for **10'**, a value of 2.8° was obtained, agreeing with the trend of the experimental results, in that **10** exhibits a higher order parameter than **5**. The rod-like natures of **5'** and **10'**, quantified by their calculated aspect ratios listed in Table 4, are consistent with the positive and relatively high experimental dichroic order parameters of **5** and **10**. As for VHF structure **16'**, the results of the calculations were found to be more complicated because four major conformers/configurations of **16'** were possible (Figure 7), dependent on the position of the alkyloxyphenyl substituent on the seven-membered ring and the s-*cis*/s-*trans* conformers of the exocyclic "butadiene" parts. The calculated energies indicate that the s-*trans* conformers are more stable than the s-*cis* conformers, and that the s-*trans E*-VHF **16'c** is the most stable of the VHF structures.

The calculated properties for **5'**, **10'** and the four structures of VHF **16'** are given in Table 4. The relatively rod-like natures of **16'a-b** which are quantified by aspect ratios of 2.2-2.5, combined with calculated angles of *ca.* 21-25° between the TDM vectors and the minimum MOI axes, are indicative of compounds that may be expected to exhibit positive and relatively high dichroic order parameters in an aligned liquid crystal host. In contrast, the aspect ratios of **16'c-d** are both close to 1, suggesting that the molecular alignment, and therefore the dichroic order parameters, of these structures would be low. The lower calculated energies of **16'c-d** than **16'a-b** (Figure 7) suggest **16'c-d** would be the dominant structures at room temperature, which is consistent with the low experimental order parameters measured after irradiation of **5** and **10** (Table 3). This result was not unexpected, as when the s-*cis* conformer is formed it can close rapidly to the DHA, and therefore s-*cis* conformers are merely transient and do not accumulate when VHF **16** has been generated during the irradiation process. This is reflected by the extremely fast rate of back reaction when the VHF had been locked in this conformation.[16]

Table 4. Calculated transition wavelengths (λ), oscillator strengths (f), angles (β) between the TDM and minimum MOI axes, and aspect ratios for DHAs **5'** and **10'** and VHF structures **16'a-d'**. The longest wavelength transitions with $f > 0.2$ are listed.

Structure	λ / nm	f	β / °	Aspect ratio
5'	358	0.85	9.4	2.12
10'	378	1.29	2.8	2.89
16'a	432	0.31	20.9	2.49
16'b	417	0.82	24.5	2.21
16'c	405	1.00	39.3	1.39
16'd	400	0.85	16.9	0.88

Liquid Crystal Properties of Azulenes 6 and 14. Unlike the DHAs employed in this study, their corresponding azulenes were thermally stable and their liquid-crystalline properties could be measured in their neat forms. Yet, the bent structure **6** did not exhibit a liquid crystalline phase, nor did its corresponding DHA precursor **5**. On the other hand, linear azulene **14** exhibited liquid crystalline phases with transition temperatures, enthalpy and entropy values summarized in Figure 8, and the DSC thermogram is shown in Figure 9. This material melted into a smectic A phase at 138 °C. This phase has a large temperature range of 185 °C before the transition into a nematic phase occurred at 323 °C. These transitions occurred at very high temperatures, and a little decomposition was observed when analyzing the material from the DSC pan by ^{1}H NMR spectroscopy after three cycles of heating to as high as 360 °C.

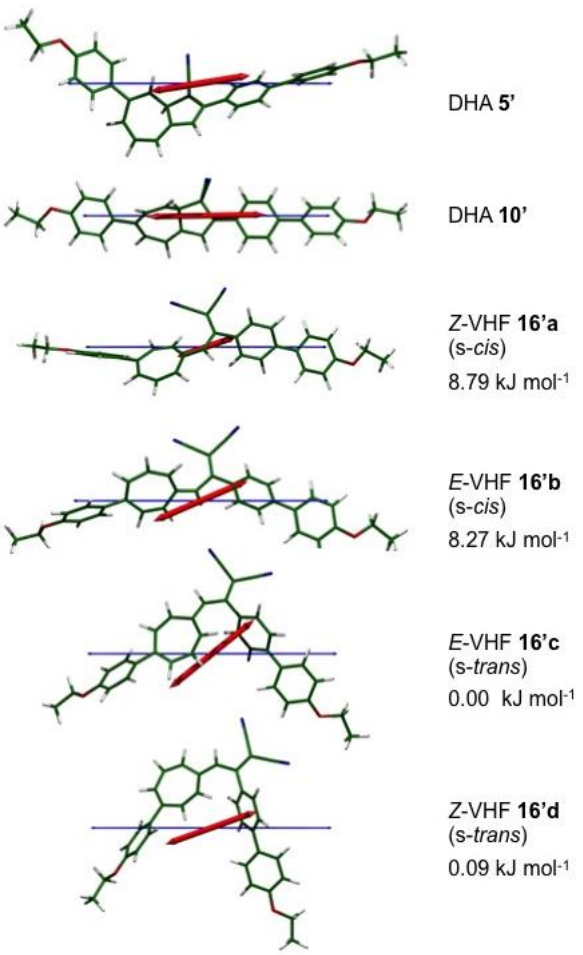

Figure 7. DFT optimised structures of **5'**, **10'** and **16'a-d** (ethoxy-substituted analogues of **5**, **10**, and **16a-d**) showing the TDM vectors associated with the calculated transitions listed in Table 4 (red arrows) and the minimum MOI axes (blue arrows). Calculated relative energies of **16'a-d** are also shown.

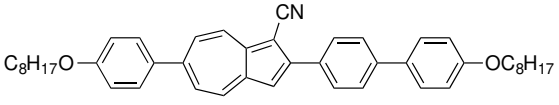

14

Cr 138.4 SmA 323.3 N 333.0 Iso

Iso 332.0 N 322.1 SmA 116.0 Cr

Figure 8. Transition temperatures (°C) for azulene **14**.

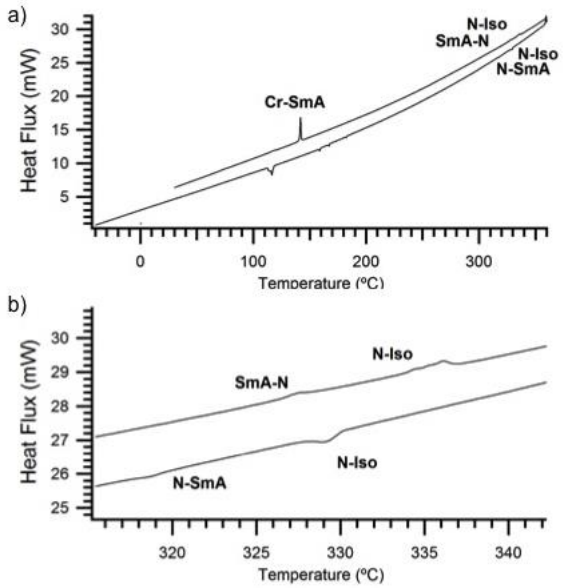

Figure 9. a) DSC thermograms with heating-cooling rate of 10 °C min^{-1} for compound **14**. b) Zoom of the DSC.

When examining **14** under POM around 340 °C (measured from the heating mantle), a focal conic texture was observed. Some areas had this texture, which can be seen in Figure 10a, and other areas were homogenously aligned giving black areas. From this, it was possible to conclude that it was a smectic A phase. If the sample was heated further, a nematic phase appeared, giving a Schlieren texture, which is shown in Figure 10b. If the glass slide was removed from the heat, and quickly examined under the microscope, a third phase could be observed, shown in Figure 10c. The third phase was identified as a Smectic C phase due to the observation of both a Schlieren texture and focal-conic defects The reason we do not see this in the DSC is that the phase transition occurred under the melting point of **14**, which also meant that shortly after the slide was removed from the heat, the material crystallized.

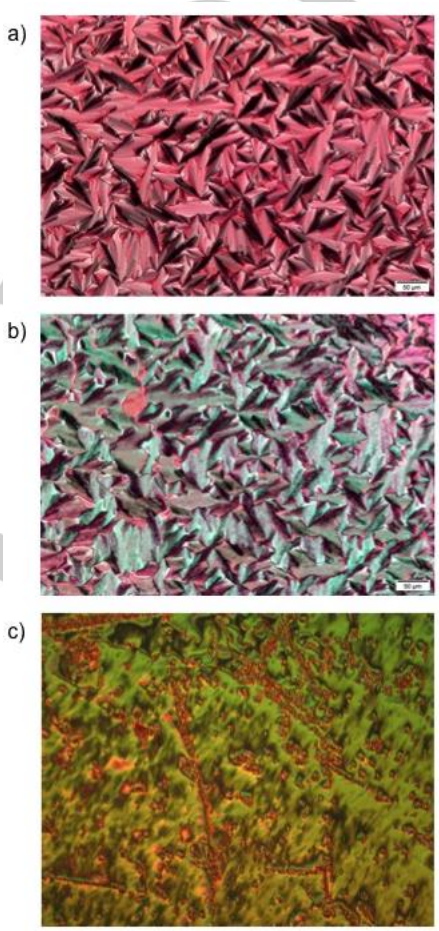

Figure 10. POM images of **14** showing a) the smectic A phase at 340 °C, b) the nematic phase at 349 °C, c) the smectic C phase at super cooling.

Photophysical Properties of Azulenes. Azulenes **6** and **14** have two different conjugation patterns, which affected the color of these materials. While bent molecule **6** appeared blue, linearly shaped azulene **14** appeared maroon in color. In the absorbance spectra in 1,2-dichloroethane, the difference appeared as a peak at 440 nm for **14**, where **6** clearly exhibited a shoulder around 420 nm (Figure 11a). As both azulenes are highly colored, the obvious use was as dopants in a guest-host system. Therefore azulenes **6** and **14** were doped into host **15**, and the absorption spectra were measured with the light parallel and perpendicular to the alignment of the cell (Figure 11b). Azulene **6** had an order parameter of $S = 0.71$, while the order parameter for azulene **14** was determined to be $S = 0.75$. These are much higher order parameters than the formerly reported

results for azulenes, where the order parameter is around S = 0.3,[21] which shows that with the right substitution pattern azulenes are promising candidates for guest-host systems.

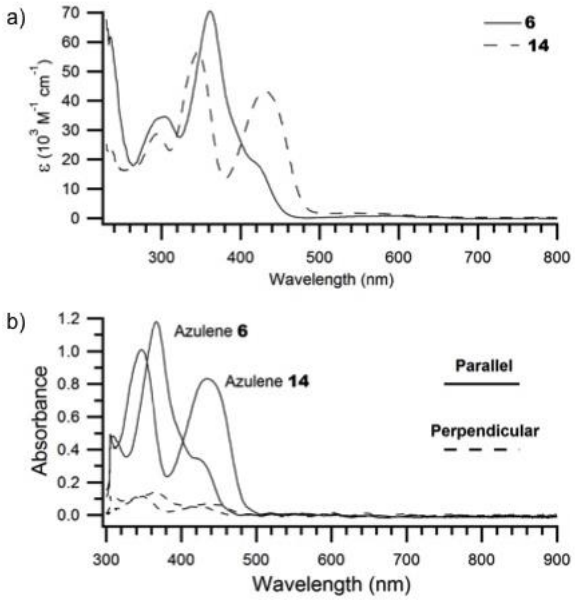

Figure 11. a) UV-Vis absorption spectra of azulenes **6** and **14** in 1,2-dichloroethane. b) UV-Vis absorption spectra in liquid crystal host **15** with the light polarized parallel and perpendicular to alignment of **6** and **14**.

DFT calculations were done in the same manner for **6** and **14** as for DHA **5** and **10**, in order to find the angles, β, between the TDM and minimum MOI axes and their aspect ratios (Figure 12; Table 5). For **6'** (the ethoxy analogue of **6**) the angle was found to be 4.1° and the aspect ratio found to be 1.96 which is consistent with the high experimental order parameter. For **14'** (the ethoxy analogue of **14**), the angle was calculated to be 3.1° and the aspect ratio calculated as 2.36 which again is consistent with the experimental order parameters, showing a slightly higher order parameter for **14** compared to **6**. In order to incorporate these systems into devices, the aim is a higher order parameter, ideally approaching 1. To obtain this, the angle between TDM and MOI should be as small as possible.

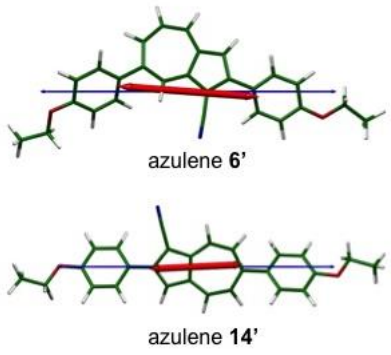

Figure 12. DFT optimized structures of **6'** and **14'** (ethoxy-substituted analogues of **6** and **14**) showing the TDM vectors associated with the calculated transitions (red arrows) and the minimum MOI axes (blue arrows).

Table 5. Calculated transition wavelengths (λ), oscillator strengths (f), angles (β) between the TDM and minimum MOI axes, and aspect ratios for azulenes **6'**, **14'**, and **18**-**21**. The longest wavelength transitions with $f > 0.2$ are listed.

Compound	λ / nm	f	β / °	Aspect ratio
6'	313	1.55	4.1	1.96
14'	383	0.62	3.1	2.36
18	321	1.65	4.5	1.99
19	388	0.66	0.2	2.31
20	294	1.78	2.6	1.99
21	379	0.65	0.2	3.29

An alternative approach could be to incorporate an additional cyano group into the 3-position, giving a higher amount of symmetry to the molecule. Such structures are shown in Figure 13, along with the calculated visible TDM vectors (see data in Table 5). Azulene **18** has an angle of β = 4.5°, which is not so different from that of **6** and **14**. By contrast, **19** has a significantly smaller angle of β = 0.2°, which suggests that this analogue should give a high order parameter. Another possibility could be to exchange the cyano group at the 2-position with a hydrogen atom to give structures **20** and **21** (Figure 13). These exhibit the same trend as **18** and **19**. For the 7-substituted system **20**, the angle, β, was calculated to be 2.6°, whilst for the 6-substituted system **21**, the angle was 0.2°. Further, the aspect ratios of compounds **19** and **21** are higher than those of **18** and **20**. These results give a clear indication that the 6-substituted azulenes are interesting molecules for future work.

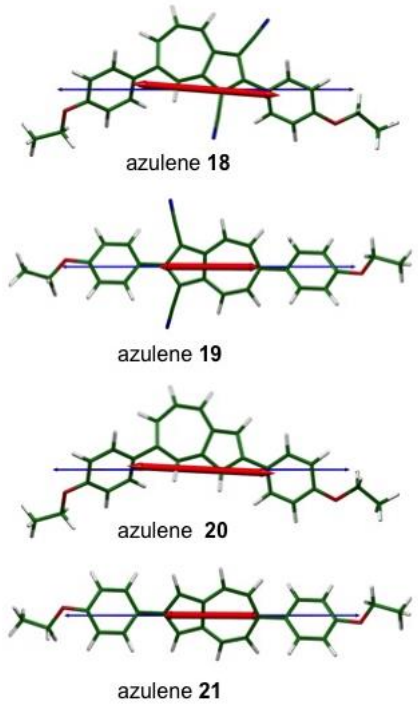

Figure 13. DFT optimized structures of azulenes **18**, **19**, **20**, and **21** (from top to bottom) showing the TDM vectors associated with the calculated TDMs (red arrows) and minimum MOI axes (blue arrows).

Conclusions

In conclusion, we have shown that the substitution pattern on the seven-membered ring of DHA has significant consequences for its liquid crystalline properties. We have managed to isolate both 6- and 7-substituted DHA derivatives on a preparative scale, rather than just as a mixture of isomers, which has allowed for thorough investigations. Thus, whereas substitution on position 7 provides a bent structure that did not result in liquid crystallinity, substitution on position 6 provides a more rod-like structure with liquid crystalline properties. When measuring the DHAs in a nematic host system, they showed good alignment, giving high dichroic order parameters. Interestingly, the order parameters were lowered significantly upon irradiation resulting in conversion to the VHF forms. The ability of the system to overwrite by irradiation means that it is promising for future devices. In addition a highly coloured and relatively stable azulene derivative could be formed directly from the DHA, and it also showed promising results as a dye for guest-host systems, giving a higher order parameter than those previously reported for azulenes. The DFT calculations reported here provide a rationale for the observed order parameters of the dyes and additionally enabled identification of suitable molecules for future synthesis and study.

Experimental Section

General Methods. Chemicals were used as purchased from commercial sources. Purification of products was carried out by flash chromatography on silica gel (40−63 μm, 60 Å). Thin-layer chromatography (TLC) was carried out using aluminum sheets precoated with silica gel. ^{1}H NMR (500 MHz) and ^{13}C NMR (125 MHz) spectra were recorded on a Bruker 500 MHz instrument with a non-inverse cryoprobe using the residual solvent as the internal standard ($CDCl_3$, ^{1}H 7.26 ppm and ^{13}C 77.16 ppm). All chemical shifts are quoted on the δ scale (ppm), and all coupling constants (*J*) are expressed in Hz. In APT spectra, CH and CH_3 correspond to negative signals and C and CH_2 correspond to positive signals. High resolution mass spectra (HRMS) were acquired using matrix assisted laser desorption ionisation (MALDI). Melting points are uncorrected. All solution based spectroscopic measurements were performed in a 1-cm path length cuvette. Photoswitching experiments were performed using a Vilber Lourmet TLC lamp with a wavelength at 365 nm at 610 μw/cm^3. The thermal back reaction was measured by heating the sample (cuvette) by a Peltier unit in the UV-Vis spectrophotometer. UV-Vis absorption measurements on liquid crystals were performed scanning the region 900-190 nm, and the thermal back reaction was followed at ambient temperature. Dielectric measurements were done on an INSTEC ALCT Property Tester. Compound **8**[18] was made by its literature method. Density functional theory (DFT) optimisations and time-dependent DFT (TD-DFT) calculations were carried out on isolated molecules at the CAM-B3LYP/cc-pVDZ level using Gaussian 09.[23] Calculated energies referred to in the text correspond to the Gibbs energies calculated for the optimized structures. Minimum moment of inertia (MOI) axes were calculated as the eigenvectors associated with the minimum eigenvalues of the diagonalised moment of inertia tensors of the geometries studied. Each molecular length was determined as the length of the van der Waals molecular surface along the minimum MOI axis, and each molecular width was calculated as twice the maximum perpendicular distance from the minimum MOI axis to the van der Waals molecular surface. Each molecular aspect ratio was calculated as the ratio of the molecular length to the molecular width.

Synthetic Protocols

2-(4'-(Octyloxy)-[1,1'-biphenyl]-4-yl)-7-(4-(octyloxy)phenyl)azulene-1,1(8a*H*)-dicarbonitrile (5): To a stirring solution of **8** (1.07 g, 2.80 mmol) in CH_2Cl_2 (25 mL), under an argon atmosphere at -78 °C was added dropwise over 5 min a solution of Br_2 (3.9 mL, 0.78M in CH_2Cl_2, 3.1 mmol), and the contents of the vessel were allowed to stir for 4 h. The vessel was directly subjected to rotary evaporation, without the use of a water bath, and when dry, the contents were dissolved in THF (50 mL). The vessel was cooled in an ice bath and to this stirring solution was added a solution of LiHMDS (3.1 mL, 1M in toluene, 3.1 mmol), and the mixture was allowed to stir for 1 h in the ice bath and then a further hour after the bath had been removed. The reaction was quenched using saturated aqueous NH_4Cl (20 mL) and diluted with water (20 mL), and the mixture was extracted with Et_2O (3 x 50 mL). The combined organic phase was dried over $MgSO_4$, filtered and the solvent removed *in vacuo*.

The residue was taken up in toluene (60 mL) and water (10 mL) and the mixture degassed. To the stirring biphasic mixture were added (4-(octyloxy)phenyl)boronic acid (2.56 g, 10.2 mmol), K_3PO_4 (4.19 g, 19.7 mmol), $Pd(OAc)_2$ (32 mg, 0.14 mmol) and RuPhos (140 mg, 0.30 mmol), and the resulting mixture was allowed to stir at ambient temperature for 20 h. The contents of the flask were diluted with saturated aqueous NH_4Cl (40 mL), water (40 mL), and toluene (50 mL). The phases were separated and the aqueous phase was extracted with toluene (50 mL). The combined organics were dried over $MgSO_4$, filtered and the solvent removed *in vacuo*. The crude residue was purified by flash column chromatography (gradient elution of 50% toluene/heptane to 70% toluene/heptane) to give an orange oil which was crystalized from CH_2Cl_2/EtOH to afford **5** (940 mg, 45%) as a fluffy yellow solid. R_f=0.31 (60% toluene/heptane). M.p. = 118-137 °C. ^{1}H NMR (500 MHz, $CDCl_3$): δ = 7.80 (d, J = 8.6 Hz, 2H), 7.66 (d, J = 8.6 Hz, 2H), 7.56 (d, J = 8.8 Hz, 2H), 7.33 (d, J = 8.8 Hz, 2H), 6.99 (d, J = 8.8 Hz, 2H), 6.91 (s, 1H), 6.88 (d, J = 8.8 Hz, 2H), 6.80 (dd, J = 11.5, 5.8 Hz, 1H), 6.75 (d, J = 11.5 Hz, 1H), 6.35 (br d, J = 5.8 Hz, 1H), 5.94 (d, J = 4.6 Hz, 1H), 4.01 (t, J = 6.6 Hz, 2H), 3.97 (t, J = 6.6 Hz, 2H), 3.82 (dd, J = 4.6, 1.6 Hz, 1H), 1.83-1.76 (m, 4H), 1.51–1.43 (m, 4H), 1.37–1.29 (m, 16H), 0.90 (t, J = 7.0 Hz, 3H), 0.88 (t, J = 7.0 Hz, 3H) ppm. ^{13}C NMR (125 MHz, $CDCl_3$): δ = 159.50, 159.36, 142.64, 141.01, 140.96, 139.37, 132.61, 132.49, 132.33, 132.13, 131.08, 129.03, 128.72, 128.22, 127.39, 126.86, 120.08, 115.47, 115.13, 114.75, 114.61, 113.25, 68.31, 68.26, 51.09, 45.10, 31.98, 29.52, 29.52, 29.42, 29.40, 26.22, 26.19, 22.82, 22.82, 14.26 ppm, 4Cs masked. HRMS (MALDI +ve) calcd for $C_{46}H_{52}N_2O_2$ [$(M)^{\cdot+}$]: m/z = 664.4023; exp 664.4029.

2-([1,1'-Biphenyl]-4-yl)-7-phenylazulene-1,1(8a*H*)-dicarbonitrile (7): To a stirring solution of **8** (1.07 g, 2.80 mmol) in CH_2Cl_2 (25 mL) at –78 °C was added dropwise a solution of Br_2 in CH_2Cl_2 (3.9 mL, 0.78M, 3.1 mmol), and the resulting solution was stirred for 4 h. The cold bath was removed, and the solvent was immediately removed under reduced pressure. The crude mixture was dissolved in THF (50 mL) and cooled in an ice bath. To this stirring solution was added a solution of LiHMDS (3.1 mL, 1M in toluene, 3.1 mmol), and the contents of the vessel were allowed to stir 1 h. The reaction was quenched by the addition of saturated aqueous NH_4Cl (20 mL), followed by water (20 mL), and the mixture was extracted with Et_2O (3 x 50 mL). The combined ethereal extracts were dried over $MgSO_4$, filtered and the solvent removed *in vacuo*. The crude residue was taken up in toluene (60 mL) and water (10 mL) and degassed with argon before adding phenyl boronic acid (1.03 g, 4.26 mmol), K_3PO_4 (2.73 g, 12.9 mmol), $Pd(OAc)_2$ (64 mg, 0.29 mmol) and RuPhos (264 mg, 0.57 mmol) to the vessel. The biphasic mixture was stirred for 24 h at 80 °C. The contents of the vessel were diluted with water (100 mL) and the phases were separated. The aqueous phase was extracted with toluene (2 x 50 mL) and the combined organics dried over $MgSO_4$, filtered and the solvent removed by rotary evaporation. The crude residue was subjected to flash column chromatography (gradient elution of 40% toluene/heptane to toluene) affording the DHA **7**, which was then crystalized from CH_2Cl_2/heptane to give **7** (234 mg, 20%) as a yellow crystalline solid. In addition, 2-([1,1'-biphenyl]-4-yl)azulene-1-carbonitrile (55 mg, 6%) as a dark blue solid and 2-([1,1'-biphenyl]-4-yl)-7-phenylazulene-1-carbonitrile (72 mg, 7%) as a dark green solid could be isolated during the course of the chromatography. **(7):** R_f=0.21 (40% toluene/heptane). M.p. = 181-211 °C (decomposes). ^{1}H NMR (500 MHz, $CDCl_3$): δ = 7.87 (d, J = 8.4 Hz, 2H), 7.74 (d, J = 8.4 Hz, 2H), 7.68–7.64 (m, 2H), 7.54–7.47 (m, 2H), 7.46–7.36 (m, 6H), 6.97 (s, 1H), 6.88–6.78 (m, 2H), 6.41 (d, J = 5.9 Hz, 1H), 6.05 (d, J = 4.7 Hz, 1H), 3.89 (dd, J = 4.7, 1.6 Hz, 1H) ppm. ^{13}C NMR (125 MHz, $CDCl_3$): δ = 143.00, 140.93, 140.75, 140.18, 140.00, 139.93, 132.55, 132.20, 131.50, 129.40, 129.12, 128.71, 128.20, 128.18, 128.00, 127.84, 127.19, 126.89, 120.37, 116.30, 115.37, 113.15, 51.10, 45.13 ppm. HRMS (MALDI +ve) calcd for $C_{30}H_{20}N_2$ [$(M)^{\cdot+}$]: m/z = 408.1621; exp 408.1628. Analysis calcd (%) for $C_{30}H_{20}N_2$: C 88.21, H 4.94 N 6.86; found: C 88.40, H 4.66, N 6.82. **2-([1,1'-Biphenyl]-4-yl)azulene-1-carbonitrile:** R_f=0.33 (toluene). ^{1}H NMR (500 MHz, $CDCl_3$): δ = 8.63 (d, J = 9.7 Hz, 1H), 8.40 (d, J = 9.5 Hz, 1H), 8.16 (d, J = 8.3 Hz, 2H), 7.79–7.75 (m, 3H), 7.03–7.67 (m, 2H), 7.58 (s, 1H), 7.56–7.45 (m, 4H), 7.43–7.37 (m, 1H) ppm. HRMS (MALDI +ve) calcd for $C_{30}H_{20}N_2$ [$(M)^{\cdot+}$]: m/z = 305.1199; exp 305.1208. Data in accordance with literature.[24] **2-([1,1'-Biphenyl]-4-yl)-7-phenylazulene-1-carbonitrile:** R_f=0.49 (toluene). M.p. > 230 °C. ^{1}H NMR (500 MHz, $CDCl_3$): δ = 8.90 (d, J = 1.8 Hz, 1H), 8.39 (d, J = 9.8 Hz, 1H), 8.19 (d, J = 8.2 Hz, 2H), 8.01 (ddd, J = 10.3, 1.8, 0.8 Hz, 1H), 7.78 (d, J = 8.3 Hz, 2H), 7.71–7.68 (m, 4H), 7.58 (s, 1H), 7.58–7.44 (m, 6H), 7.43–7.37 (m, 1H) ppm. ^{13}C NMR (125 MHz, $CDCl_3$): δ = 152.30, 145.24, 143.51, 142.55, 142.41, 141.80, 140.44, 139.07, 136.80, 136.46, 133.38, 129.24, 129.21, 129.07, 128.61, 128.24, 127.96, 127.93, 127.66, 127.26, 118.44, 116.27, 94.92 ppm. HRMS (MALDI +ve) calcd for $C_{29}H_{19}N$ [$(M)^{\cdot+}$]: m/z = 382.1590; exp 382.1600. Analysis calcd (%) for $C_{29}H_{19}N$: C 91.31, H 5.02 N 3.67; found: C 91.18, H 4.84, N 3.56.

Heating Experiments of DHAs 5 and 7 (Scheme 3 and Table 1)

Entry 1: Under an argon atmosphere, in a sealed microwave tube, compound **7** (53 mg, 0.13 mmol) was heated conventionally to 110 °C for 1 week. This resulted in the exclusive transformation to **13** (53 mg, 100%).

Entry 2: DHA **7** (20 mg, 0.49 mmol) was heated conventionally under an argon atmosphere to 140 °C for 4 h and 40 min in a sealed microwave vial. This resulted in the formation of a mixture of **12** and **13** in the ratio 5:6. The material was subjected to flash column chromatography (13% EtOAc/heptane), and it was possible to obtain pure samples of **12** (6 mg, 30%) as a yellow solid and **13** (6 mg, 30%) also a yellow solid.

Entry 3: A CH_2Cl_2 (5 mL) solution of DHA **7** (57 mg, 0.14 mmol) was dried inside a microwave vial using a stream of nitrogen. The vial was sealed and placed under an argon atmosphere before being heated in an oil bath at 180 °C for 1 h. ^{1}H NMR analysis indicated the formation of **12** and **13** in a 4:1 ratio. The material was then subjected to flash column chromatography (13% EtOAc/heptane) followed by recrystallization from hot CCl_4 to give pure **12** (16 mg, 28%).

2-([1,1'-Biphenyl]-4-yl)-6-phenylazulene-1,1(8a*H*)-dicarbonitrile (12): R_f=0.34 (13% EtOAc/heptane). M.p. = 221-223 °C. ^{1}H NMR (500 MHz, $CDCl_3$): δ = 7.85 (d, J = 8.3 Hz, 2H), 7.72 (d, J = 8.3 Hz, 2H), 7.65–7.63 (m, 2H), 7.50–7.47 (m, 4H), 7.43–7.38 (m, 3H), 7.37–7.34 (m, 1H), 6.99 (s, 1H), 6.96 (d, J = 6.9 Hz, 1H), 6.56 (d, J = 10.4 Hz, 1H), 6.48 (dd, J = 6.9, 1.8 Hz, 1H), 6.04 (dd, J = 10.4, 4.2 Hz, 1H), 3.86 (ddd, J = 4.2, 1.8, 1.8 Hz, 1H) ppm. ^{13}C NMR (125 MHz, $CDCl_3$): δ = 143.09, 142.87, 141.33, 139.97, 139.94, 139.13, 131.92, 129.46, 129.12, 128.86, 128.83, 128.24, 128.20, 128.16, 128.00, 127.18, 126.83, 120.97, 120.22, 115.32, 112.98, 51.10, 45.06 ppm, 1C masked. HRMS (MALDI +ve) calcd for $C_{30}H_{21}N_2$ [$(M+H)^{+}$]: m/z = 409.1699; exp 409.1711.

2-([1,1'-Biphenyl]-4-yl)-7-phenylazulene-1,1(6*H*)-dicarbonitrile (13): R_f=0.28 (13% EtOAc/heptane). M.p. > 230 °C. ^{1}H NMR (500 MHz, $CDCl_3$): δ = 7.84 (d, J = 8.5 Hz, 2H), 7.72 (d, J = 8.5 Hz, 2H), 7.67–7.59 (m, 4H), 7.48 (t, J = 7.6 Hz, 2H), 7.46–7.34 (m, 4H), 7.22 (s, 1H), 7.08 (s, 1H), 6.61 (d, J = 9.2 Hz, 1H), 5.69 (dt, J = 9.2, 7.3 Hz, 1H), 3.08 (d, J = 7.3 Hz, 2H) ppm. ^{13}C NMR (125 MHz, $CDCl_3$): δ = 144.94, 142.32, 140.07, 139.73, 138.30, 137.82, 134.02, 133.71, 129.10, 129.07, 128.91, 128.75, 128.11, 128.05, 127.95, 127.16, 126.19, 123.83, 123.73, 117.31, 113.00, 44.59, 32.02 ppm. HRMS (MALDI +ve) calcd for $C_{30}H_{21}N_2$ [$(M+H)^{+}$]: m/z = 409.1699; exp 409.1698. Analysis calcd (%) for $C_{30}H_{20}N_2$: C 88.21, H 4.94, N 6.86; found: C 88.14, H 4.77, N 6.85.

Entry 4: Under an argon atmosphere, compound **5** (99 mg, 0.15 mmol) was heated conventionally to 110 °C for 40 h in a sealed microwave tube. This resulted in the formation of a mixture of **10** and **11** in the ratio 5:1. The material was then subjected to column chromatography (gradient elution of 60% toluene/heptane to toluene) to give **10** (85 mg, 86%).

Entry 5: Under an argon atmosphere, **5** (80 mg, 0.12 mmol) was heated conventionally to 140 °C for 24 h in a sealed microwave tube. The mixture was subjected to column chromatography (75% toluene/heptane) to give **11**, a mixture of **5** and **10**, and a mixture containing all three components. The fractions containing all three components were subjected to a second flash column (60% toluene/heptane), where compound **11** was separated from photoactive DHAs **5** and **10**. All combined fractions containing **11** were recrystallized to give this product (13 mg, 16%) as a bright yellow solid. The combined components containing photoactive DHAs **5** and **10** were also recrystallized to give a mixture of **5**/**10** in a ratio of 3:7 (19 mg, 24%).

Entry 6: Compound **5** (18 mg, 0.03 mmol) was conventionally heated to 175 °C for 1 h under an argon atmosphere in a vial suitable for microwave reactions. The resulting material was subjected to flash column chromatography (gradient elution of 60% toluene/heptane to toluene). The first yellow component was collected and subsequently recrystallized from CH_2Cl_2/EtOH giving **11** (1.2 mg, 7%) as a yellow solid.

2-(4'-(Octyloxy)-[1,1'-biphenyl]-4-yl)-6-(4-(octyloxy)phenyl)azulene-1,1(8a*H*)-dicarbonitrile (10): R_f = 0.49 (60% toluene/heptane). M.p. = 154-159 °C. ^{1}H NMR (500 MHz, $CDCl_3$): δ = 7.80 (d, J = 8.3 Hz, 2H), 7.66 (d, J = 8.3 Hz, 2H), 7.56 (d, J = 8.5 Hz, 2H), 7.40 (d, J = 8.5 Hz, 2H), 6.99 (d, J = 8.5 Hz, 2H), 6.95 (s, 1H), 6.92 (d, J = 8.5 Hz, 2H), 6.89 (d, J = 7.0 Hz, 1H), 6.51 (d, J = 10.3 Hz, 1H), 6.44 (dd, J = 7.0, 1.7 Hz, 1H), 6.01 (dd, J = 10.3, 4.3 Hz, 1H), 4.01 (t, J = 6.5 Hz, 2H), 3.99 (t, J = 6.5 Hz, 2H), 3.83 (ddd, J = 4.3, 1.7, 1.7 Hz, 1H), 1.84 – 1.77 (m, 4H), 1.51–1.44 (m, 4H), 1.42–1.24 (m, 16H), 0.91–0.88 (m, 6H) ppm. ^{13}C NMR (125 MHz, $CDCl_3$): δ = 159.33, 159.28, 142.37, 139.46, 138.52, 133.95, 133.47, 132.01, 131.44, 128.68, 128.66, 128.05, 127.23, 126.60, 120.76, 119.91, 119.34, 115.27, 115.17, 114.98, 114.64, 112.93, 68.43, 68.16, 50.98, 44.86, 31.83, 31.78, 29.38, 29.37, 29.28, 29.26, 29.20, 28.98, 26.07, 26.05, 25.94, 22.67, 22.65, 14.11 ppm. HRMS (MALDI +ve) calcd for $C_{46}H_{53}N_2O_2$ [$(M+H)^+$]: m/z = 665.4102; exp 665.4101. Analysis calcd (%) for $C_{46}H_{52}N_2O_2$ (664.40): C 83.09, H 7.88, N 4.21; found: C 82.96, H 7.89, N 4.24.

2-(4'-(Octyloxy)-[1,1'-biphenyl]-4-yl)-7-(4-(octyloxy)phenyl)azulene-1,1(6*H*)-dicarbonitrile (11): R_f=0.51 (60% toluene/heptane). M.p. = 174-175.5 °C. ^{1}H NMR (500 MHz, $CDCl_3$): δ = 7.79 (d, J = 8.4 Hz, 2H), 7.67 (d, J = 8.4 Hz, 2H), 7.57 (d, J = 8.8 Hz, 2H), 7.56 (d, J = 8.8 Hz, 2H), 7.18 (s, 1H), 7.01 (s, 1H), 7.00 (d, J = 8.8 Hz, 2H), 6.92 (d, J = 8.8 Hz, 2H), 6.58 (d, J = 9.2 Hz, 1H), 5.62 (dt, J = 9.2, 7.2 Hz, 1H), 4.02 (t, J = 6.2 Hz, 2H), 4.00 (t, J = 6.2 Hz, 2H), 3.04 (d, J = 7.2 Hz, 2H), 1.91–1.73 (m, 4H), 1.50–1.44 (m, 4H), 1.42–1.23 (m, 16H), 0.93–0.84 (m, 6H) ppm. ^{13}C NMR (125 MHz, $CDCl_3$): δ = 159.85, 159.38, 143.99, 141.85, 138.00, 137.85, 133.76, 132.87, 132.33, 131.93, 129.38, 128.49, 128.16, 127.51, 126.08, 123.78, 123.14, 115.76, 115.11, 114.82, 113.20, 68.36, 68.31, 44.57, 31.98, 31.97, 31.90, 29.86, 29.53, 29.51, 29.43, 29.41, 29.40, 29.37, 26.22, 26.18, 22.82, 14.26 ppm, 1C masked. HRMS (MALDI +ve) calcd for $C_{46}H_{52}N_2O_2$ [$(M)^{+}$]: m/z = 664.4023; exp 664.4029.

2-(4'-(Octyloxy)-[1,1'-biphenyl]-4-yl)-7-(4-(octyloxy)phenyl)azulene-1-carbonitrile (6): To a solution of **5** (78 mg, 0.117 mmol) in toluene (3 mL) was added DBU (0.1 mL, 6.7 mmol), and the resulting solution was stirred at ambient temperature for 2 h. The reaction was quenched with aqueous HCl (2M, 10 mL), and the mixture was extracted with CH_2Cl_2 (4 x 20 mL). The combined organics were dried through a pad of cotton and the solvent was removed under reduced pressure. The residue was subjected to flash column chromatography (gradient elution of 13% toluene/heptane to 70% toluene/heptane) and recrystallized from CH_2Cl_2/EtOH to give pure **6** (24 mg, 32%) as a blue-green solid. R_f=0.38 (60% toluene/heptane). M.p. = 165.5-167.5 °C. ^{1}H NMR (500 MHz, $CDCl_3$): δ = 8.87 (d, J = 1.8 Hz, 1H), 8.34 (d, J = 9.8 Hz, 1H), 8.16 (d, J = 8.3 Hz, 2H), 7.98 (ddd, J = 10.4, 1.8, 0.7 Hz, 1H), 7.73 (d, J = 8.3 Hz, 2H), 7.63 (d, J = 8.8 Hz, 2H), 7.61 (d, J = 8.8 Hz, 2H), 7.55–7.46 (m, 2H), 7.05 (d, J = 8.8 Hz, 2H), 7.01 (d, J = 8.8 Hz, 2H), 4.05 (t, J = 6.5 Hz, 2H), 4.02 (t, J = 6.6 Hz, 2H), 1.88–1.78 (m, 4H), 1.53–1.46 (m, 4H), 1.42–1.31 (m, 16H), 0.90 (t, J = 7.0 Hz, 3H), 0.90 (t, J = 6.9 Hz, 3H) ppm. ^{13}C NMR (125 MHz, $CDCl_3$): δ = 159.41, 159.18, 152.22, 145.22, 142.50, 141.91, 141.43, 138.35, 136.05, 135.91, 135.52, 132.61, 132.53, 129.61, 129.01, 128.11, 127.47, 127.25, 118.50, 115.68, 115.14, 114.95, 94.21, 68.27, 68.16, 31.84, 29.39, 29.30, 29.27, 26.08, 26.07, 22.68, 14.12 ppm, 6Cs masked. HRMS (MALDI +ve) calcd for $C_{45}H_{51}NO_2$ [$(M)^{+}$]: m/z = 637.3914; exp 637.3920. Analysis calcd (%) for $C_{45}H_{51}NO_2$ (637.91): C 84.73, H 8.06 N 2.20; found: C 84.86, H 7.94, N 2.14.

2-(4'-(Octyloxy)-[1,1'-biphenyl]-4-yl)-6-(4-(octyloxy)phenyl)azulene-1-carbonitrile (14): Under an argon atmosphere, **5** (106 mg, 0.27 mmol) was heated conventionally in a sealed vial suitable for microwave reactions to 110 °C for 40 h. This resulted in a mixture of two compounds **10** and **11** in a ratio of 5:1. The mixture was dissolved in CH_2Cl_2 (50 mL). To this solution was added HMDS (0.5 mL, 2.4 mmol) and DBU (0.04 mL, 0.27 mmol), and the mixture was left to stir for 3 days, after which time, more DBU (0.04 mL, 0.27 mmol) was added, and the mixture was left to stir for a further day. Then the last portion of DBU (0.04 mL, 0.27 mmol) was added, and the mixture was left to stir for 5 h, after which it was quenched with 2 M HCl (20 mL) and extracted with CH_2Cl_2 (4 x 20 mL). The combined organics were filtered through cotton and the volatiles removed *in vacuo*. The residue was subjected to column chromatography (gradient elution of 75% toluene/heptane to toluene). The material was then recrystallized from CH_2Cl_2/EtOH to give pure **14** (43 mg, 42%) as a brown powder. R_f=0.29 (75% toluene/heptane). M.p. = Cr 138.4 SmA 323.3 N 333.0 Iso; Iso 332.0 N 322.1 SmA 116.0 Cr °C. ^{1}H NMR (500 MHz, $CDCl_3$): δ = 8.62 (d, J = 10.3 Hz, 1H), 8.39 (d, J = 10.4 Hz, 1H), 8.15 (d, J = 8.3 Hz, 2H), 7.74–7.72 (m, 3H), 7.68 (dd, J = 10.4, 1.4 Hz, 1H), 7.62 (d, J = 8.7 Hz, 2H), 7.61 (d, J = 8.7 Hz, 2H), 7.55 (s, 1H), 7.04 (d, J = 8.7 Hz, 2H), 7.01 (d, J = 8.7 Hz, 2H), 4.05 (t, J = 6.6 Hz, 2H), 4.02 (t, J = 6.6 Hz, 2H), 1.86–1.79 (m, 4H), 1.52–1.46 (m, 4H), 1.44–1.21 (m, 16H), 0.95–0.86 (m, 6H) ppm. ^{13}C NMR (125 MHz, $CDCl_3$): δ = 160.24, 159.29, 152.61, 150.99, 144.40, 141.81, 141.05, 137.01, 136.19, 134.83, 132.91, 132.71, 130.05, 129.01, 128.26, 128.24, 127.86, 127.36, 118.57, 116.48, 115.24, 115.08, 94.06, 68.43, 68.30, 31.99, 29.54, 29.53, 29.52, 29.45, 29.41, 29.41, 29.39, 14.27 ppm, 5Cs masked. HRMS (MALDI +ve) calcd for $C_{45}H_{52}NO_2$ [$(M+H)^+$]: m/z = 638.3993; exp 638.3999. Analysis calcd (%) for $C_{45}H_{51}NO_2$ (637.91): C 84.73, H 8.06 N 2.20; found: C 84.80, H 7.99, N 2.14.

Absorption maxima (λ_{max}) and extinction coefficients (ε) for selected compounds are summarized in Table 6.

Table 6. Absorption maxima (λ_{max}) and extinction coefficients (ε). For the blends, the densities are not known (therefore reported as g^{-1} cm^{-1}).

Compound	λ_{max}	ε
DHA **5**	374 nm in CH_3CN 378 nm in host **15**	30 x 10^3 M^{-1} cm^{-1} 4.38 x 10^9 g^{-1} cm^{-1} in host **15**
Azulene **6**	361 nm in DCE 367 nm in host **15**	70 x 10^3 M^{-1} cm^{-1} in DCE

DHA **7**	369 nm in CH_3CN	33 x 10^3 M^{-1} cm^{-1} in CH_3CN
DHA **10**	402 nm in CH_3CN 407 nm in host **15**	38 x 10^3 M^{-1} cm^{-1} 3.96 x 10^9 g^{-1} cm^{-1} in host **15**
11	416 nm in CH_3CN	28 x 10^3 M^{-1} cm^{-1} in CH_3CN
DHA **12**	389 nm in CH_3CN	44 x 10^3 M^{-1} cm^{-1} in CH_3CN
13	399 nm in CH_3CN	27 x 10^3 M^{-1} cm^{-1} in CH_3CN
Azulene **14**	346 nm (shoulder 431 nm) in DCE 347nm (shoulder 434 nm) in host **15**	57 x 10^3 M^{-1} cm^{-1} in DCE
VHF **16**	508 nm in CH_3CN (508 nm in host **15**)	33 x 10^3 M^{-1} cm^{-1} 3.90 x 10^9 g^{-1} cm^{-1} in host **15**
VHF **17**	492 nm in CH_3CN	43 x 10^3 M^{-1} cm^{-1} in CH_3CN

Acknowledgements

The Danish Council for Independent Research | Technology and Production Sciences (#12-126668) and University of Copenhagen are acknowledged for financial support. EPSRC grant EP/M020584/1 for the development of dyes for liquid crystal applications is acknowledged.

Keywords: Dyes/Pigments • Electrocyclic reactions • Fused-ring systems • Liquid crystals • Photochromism

[1] H. Dürr, H. Bouas-Laurent, *Photochromism: Molecules and Systems*, Elsevier, Amsterdam, **1990**.

[2] a) Y. Li, A. Urbas, Q. Li, *J. Am. Chem. Soc.* **2012**, *134*, 9573-9576; b) T. Ikeda, O. Tsutsumi, *Science* **1995**, *268*, 1873-1875; c) R. H. Berg, S. Hvilsted, P. S. Ramanujam, *Nature* **1996**, *383*, 505-508; d) A. S. Matharu, S. Jeeva, P. S. Ramanujam, *Chem. Soc. Rev.* **2007**, *36*, 1868-1880; e) T. J. Bunning, R. L. Crane, W. W. Adams, *Adv. Mater. Opt. Electron.* **1992**, *1*, 293-297; f) A. Y. Bobrovsky, N. I. Boiko, V. P. Shibaev, *Adv. Mater.* **1999**, *11*, 1025-1028.

[3] G. Soula, Y.-P. Chan, Patent US 6410754 B1, **2000**.

[4] a) M. T. Sims, L. C. Abbott, S. J. Cowling, J. W. Goodby, J. N. Moore, *Chem. Eur. J.* **2015**, *21*, 10123-10130; b) M. T. Sims, L. C. Abbott, S. J. Cowling, J. W. Goodby, J. N. Moore, *J. Phys. Chem. C* **2016**, *120*, 11151-11162.

[5] T. Yamaguchi, T. Inagawa, H. Nakazumi, S. Irie, M. Irie, *Chem. Mater.* **2000**, *12*, 869-871.

[6] E. Peeters, J. Lub, J. A. M. Steenbakkers, D. J. Broer *Adv. Mater.* **2006**, *18*, 2412-2417.

[7] L. De Sio, L. Ricciardi, S. Serak, M. La Deda, N. Tabiryand C. Umetona, *J. Mater. Chem.* **2012**, 22, 6669-6673.

[8] C. Carrasco−Vela, X. Quintana, E. Otón, M. A. Geday, J. M. Otón *Opto-Electron. Rev.* **2011**, *19*, 496-500.

[9] M. G. Debije *Adv. Funct. Mater.* **2010**, *20*, 1498-1502.

[10] Q. K. Liu, C. Beier, J. Evans, T. Lee, S. L. He, I. I. Smalyukh, *Langmuir* **2011**, *27*, 7446-7452.

[11] a) G. H. Heilmeier, L. A. Zanoni, *Appl. Phys. Lett.* **1968**, *13*, 91-92; b) R. Stannarius, H. Kresse, G. Pelzl, *Handbook of liquid crystals*, Wiley-VCH, **1998**, Vol. 2A, p. 257-302.

[12] J. Daub, T. Knöchel, A. Mannschreck, *Angew. Chem. Int. Ed. Engl.* **1984**, *23*, 960-961.

[13] S. L. Broman, S. L. Brand, C. R. Parker, M. Å. Petersen, C. G. Tortzen, A. Kadziola, K. Kilså, M. B. Nielsen, *ARKIVOC* **2011**, *ix*, 51-67.

[14] S. L. Broman, M. Jevric, M. B. Nielsen, *Chem. Eur. J.* **2013**, *19*, 9542-9548.

[15] a) S. L. Broman, M. Å. Petersen, C. G. Tortzen, A. Kadziola, K. Kilså, M. B. Nielsen, *J. Am. Chem. Soc.* **2010**, *132*, 9165-9174; b) M. Cacciarini, A. B. Skov, M. Jevric, A. S. Hansen, J. Elm, H. G Kjaergaard, K. V. Mikkelsen, M. B. Nielsen, *Chem. Eur. J.* **2015**, *21*, 7454-7461; c) A. U. Petersen, M. Jevric, J. Elm, S. T. Olsen, C. G. Tortzen, A. Kadziola, K. V. Mikkelsen, M. B. Nielsen, *Org. Biomol. Chem.* **2016**, *14*, 2403-2412; d) M. Cacciarini, M. Jevric, J. Elm, A. U. Petersen, K. V. Mikkelsen, M. B. Nielsen, *RSC Adv.* **2016**, *6*, 49003-49010.

[16] S. L. Broman, O. Kushnir, M. Rosenberg, A. Kadziola, J. Daub, M. B. Nielsen, *Eur. J. Org. Chem.* **2015**, *19*, 4119-4130.

[17] A. U. Petersen, M. Jevric, R. J. Mandle, E. J. Davis, S. J. Cowling, J. W. Goodby, M. B. Nielsen, *RSC Adv.* **2015**, *5*, 89731-89744.

[18] S. L. Broman, M. Jevric, A. D. Bond, M. B. Nielsen, *J. Org. Chem.* **2014**, *79*, 41-64.

[19] M. Å. Petersen, S. L. Broman, K. Kilså, A. Kadziola, M. B. Nielsen, *Eur. J. Org. Chem.* **2011**, *6*, 1033-1039.

[20] G. Nöll, J. Daub, M. Lutz, K. Rurack, *J. Org. Chem.* **2011**, *76*, 4859-4873.

[21] a) S. E. Estdale, R. Brettle, D. A. Dunmur, C. M. Marson, *J. Mater. Chem.* **1997**, *37*, 391-401; b) K. Praefcke, D. Z. Schmidt, *Naturforsch* **1981**, *36b*, 375-378; c) S. H. Simpson, R. M. Richardson, S. Hanna, *J. Chem. Phys.* **2007**, *127*, 104901.

[22] M. T. Sims, L. C. Abbott, S. J. Cowling, J. W. Goodby, J. N. Moore, *J. Phys. Chem. C* **2016**, *120*, 11151-11162.

[23] M. J. Frisch, G. W. Trucks, H. B. Schlegel, G. E. Scuseria, M. A. Robb, J. R. Cheeseman, G. Scalmani, V. Barone, B. Mennucci, G. A. Petersson, H. Nakatsuji, M. Caricato, X. Li, H. P. Hratchian, A. F. Izmaylov, J. Bloino, G. Zheng, J. L. Sonnenberg, M. Hada, M. Ehara, K. Toyota, R. Fukuda, J. Hasegawa, M. Ishida, T. Nakajima, Y. Honda, O. Kitao, H. Nakai, T. Vreven, J. A. Montgomery, Jr., J. E. Peralta, F. Ogliaro, M. Bearpark, J. J. Heyd, E. Brothers, K. N. Kudin, V. N. Staroverov, R. Kobayashi, J. Normand, K. Raghavachari, A. Rendell, J. C. Burant, S. S. Iyengar, J. Tomasi, M. Cossi, N. Rega, J. M. Millam, M. Klene, J. E. Knox, J. B. Cross, V. Bakken, C. Adamo, J. Jaramillo, R. Gomperts, R. E. Stratmann, O. Yazyev, A. J. Austin, R. Cammi, C. Pomelli, J. W. Ochterski, R. L. Martin, K. Morokuma, V. G. Zakrzewski, G. A. Voth, P. Salvador, J. J. Dannenberg, S. Dapprich, A. D. Daniels, Ö. Farkas, J. B. Foresman, J. V. Ortiz, J. Cioslowski, D. J. Fox, *Gaussian 09*, Revision B.01, Gaussian Inc., Wallingford CT, **2009**.

[24] S. L. Broman, S. Lara-Avila, C. L. Thisted, A. D. Bond, S. Kubatkin, A. Danilov, M. B. Nielsen, *Adv. Funct. Mater.* **2012**, *22*, 4249-4258.

Entry for the Table of Contents

FULL PAPER

Derivatives of the dihydroazulene/vinylheptafulvene photo-/thermoswitch were prepared and studied for their liquid crystalline and switching properties in liquid crystalline host systems. The properties were found to be strongly dependent on the position of a substituent group in the seven-membered ring of the dihydroazulene.

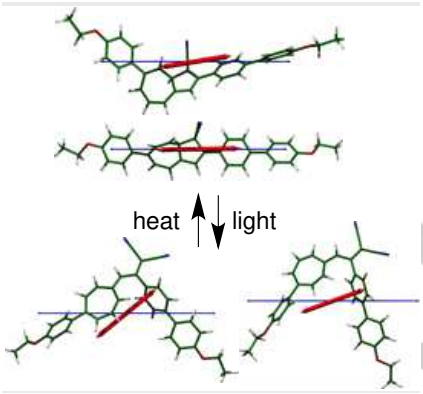

*A. U. Petersen, M. Jevric, R. J. Mandle, M. T. Sims, J. N. Moore, S. J. Cowling, J. W. Goodby, M. B. Nielsen**

Page No. – Page No.

Photoswitching of Dihydroazulene Derivatives in Liquid Crystalline Host Systems